The submitochondrial distribution of ubiquinone affects respiration in long-lived $Mclk1^{+/-}$ mice

Jérôme Lapointe, Ying Wang, Eve Bigras, and Siegfried Hekimi

Department of Biology, McGill University, Montréal H3A 1B1, Canada

Mclk1 (also known as *Coq7*) and *Coq3* code for mitochondrial enzymes implicated in the biosynthetic pathway of ubiquinone (coenzyme Q or UQ). $Mclk1^{+/-}$ mice are long-lived but have dysfunctional mitochondria. This phenotype remains unexplained, as no changes in UQ content were observed in these mutants. By producing highly purified submitochondrial fractions, we report here that $Mclk1^{+/-}$ mice present a unique mitochondrial UQ profile that was characterized by decreased UQ levels in the inner membrane coupled with increased UQ in the outer membrane. Dietary-supplemented UQ_{10} was actively incorporated in both mitochondrial membranes, and this was sufficient to reverse mutant mitochondrial phenotypes. Further, although homozygous *Coq3* mutants die as embryos like *Mclk1* homozygous null mice, $Coq3^{+/-}$ mice had a normal lifespan and were free of detectable defects in mitochondrial function or ubiquinone distribution. These findings indicate that MCLK1 regulates both UQ synthesis and distribution within mitochondrial membranes.

Introduction

Mutations in the mitochondrial hydroxylase CLK-1/MCLK1 lead to a variety of phenotypes, including increased longevity, in both *Caenorhabditis elegans* and mice (Ewbank et al., 1997; Liu et al., 2005; Lapointe et al., 2009; Wang et al., 2010). CLK-1/MCLK1 is necessary for the biosynthesis of ubiquinone (UQ). UQ is a benzoquinone with a head group capable of exchanging electrons and a side chain with a species-specific number of isoprene subunits (Bentinger et al., 2010). UQ_9 is the predominant form in *C. elegans* and in mice, with some UQ_{10} in mice as well. UQ is an electron carrier in the mitochondrial respiratory chain, in addition to many other functions (Green and Tzagoloff, 1966; Bentinger et al., 2010), such as the ability to function as an antioxidant (Sohal, 2004; Bentinger et al., 2007). All organs biosynthesize functionally sufficient amounts of UQ, which is found in every membrane of all cells (Dallner and Sindelar, 2000).

Complete loss of *Mclk1* is lethal in mice (Levavasseur et al., 2001; Nakai et al., 2001), but heterozygous $Mclk1^{+/-}$ animals are healthy and long-lived (Liu et al., 2005; Lapointe et al., 2009). Purified mitochondria from these mutants display impaired electron transport from complex I to III and from complex II to III as well as several additional related phenotypes, in particular altered reactive oxygen species (ROS) metabolism (Lapointe and Hekimi, 2008; Lapointe et al., 2009).

These observations are fully consistent with the observation that mouse cells that completely lack MCLK1 are unable to sustain UQ biosynthesis and only accumulate the UQ precursor demethoxyubiquinone (DMQ; Levavasseur et al., 2001; Nakai et al., 2001). However, no DMQ and normal levels of UQ were detected in $Mclk1^{+/-}$ mutants in spite of significantly reduced MCLK1 protein levels (Lapointe and Hekimi, 2008; Lapointe et al., 2009).

Previous quantifications of mitochondrial UQ in $Mclk1^{+/-}$ mice have been performed on standard extracts, which are considered to be contaminated by other organelles such as peroxisomes, lysosomes, and the endoplasmic reticulum (Graham, 2001c). Some of those organelles contain measurable amounts of UQ, which might have been sufficient to hide a small, but functionally significant, decrease of UQ in $Mclk1^{+/-}$ mitochondria. (Kalén et al., 1990; Tekle et al., 2002; Turunen et al., 2002).

The *Coq3* gene codes for an *O*-methyltransferase responsible for the first *O*-methyltransferase step in UQ biosynthesis, producing 3-methoxy-4-hydroxy-5-hexaprenylbenzoic acid, as well as for the final one, converting demethyl-UQH_2 into UQH_2 (Hsu et al., 1996). The phenotype resulting from the loss of this enzyme has never been reported in mice.

UQ, in the form of UQ_{10}, is extensively used as a nutritional supplement because of its antioxidant properties, principally

The Rockefeller University Press $30.00
J. Cell Biol. Vol. 199 No. 2   215–224
www.jcb.org/cgi/doi/10.1083/jcb.201203090

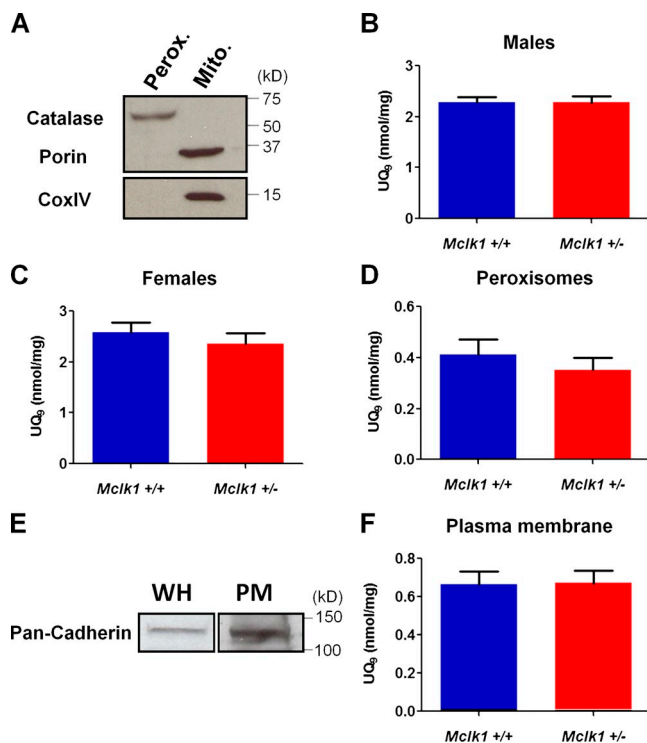JCB   215

THE JOURNAL OF CELL BIOLOGY

Figure 1. **Mitochondrial and peroxisomal ubiquinone levels are normal in *Mclk1*$^{+/-}$ mice.** (A) The purity of peroxisomal and mitochondrial fractions was assessed with antibodies against Catalase, Porin, and COXIV. (B and C) Quantification of UQ$_9$ in purified mitochondrial fractions from *Mclk1*$^{+/+}$ and *Mclk1*$^{+/-}$ mice. (D) Quantification of UQ$_9$ in purified peroxisomal fractions from *Mclk1*$^{+/+}$ and *Mclk1*$^{+/-}$ female mice. UQ$_{10}$ was not detectable in peroxisomal fractions (not depicted). (E) A representative Western blot with an anti–Pan-Cadherin antibody was used to show enrichment of this marker in plasma membrane fractions (PM) versus the whole homogenate (WH). The positions of protein molecular mass markers in the original blots are indicated in the figures in kilodaltons (kD). Both UQ$_9$ (F) and UQ$_{10}$ (not depicted) were detected in the PM, but no significant differences between genotypes could be detected. Data are the means ± SEM of 10–15 mice (error bars).

to combat aging and age-associated diseases (Sohal and Forster, 2007). Although the antiaging properties of UQ remain to be demonstrated, some beneficial actions on health in both normal and pathological conditions have been described previously (Matthews et al., 1998; Tomasetti et al., 2001; Beal, 2002; Langsjoen et al., 2005; Sohal et al., 2006; Salviati et al., 2012), including for diseases involving mitochondrial dysfunction (Dai et al., 2011). However, although most of the beneficial clinical effects of UQ$_{10}$ may be attributed to its role in mitochondrial function, little is known about the uptake of exogenous UQ$_{10}$ into individual mitochondrial membranes.

Results and discussion

The levels of UQ$_9$ and UQ$_{10}$ are unaffected in highly purified mitochondrial, peroxisomal, and plasma membrane fractions from *Mclk1*$^{+/-}$ livers

Because UQ is ubiquitously present in all cellular membranes and participates in specific functions at precise sites, its total cellular content might not be a good indicator of an excess or

deficiency at a specific location. To obtain high yields of very pure mitochondria free of contaminating organelles, we used HistoDenz-based density gradients to produce mitochondrial preparations from *Mclk1*$^{+/+}$ and *Mclk1*$^{+/-}$ mice and analyzed both UQ$_9$ and UQ$_{10}$ contents (Fig. 1 and Fig. S1). As expected, no contamination of the mitochondrial fractions by peroxisomes was detected with the peroxisomal marker Catalase (Fig. 1 A). HPLC analysis of these highly pure fractions confirmed that there is no difference between *Mclk1*$^{+/+}$ and *Mclk1*$^{+/-}$ mice in mitochondrial UQ$_9$ (Fig. 1, B and C) and UQ$_{10}$ content (Fig. S1).

Because peroxisomes might be involved in UQ biosynthesis (Tekle et al., 2002), we have also quantified UQ in peroxisomal fractions. The purity of the fractions was confirmed by the absence of the specific mitochondrial markers Porin and cytochrome *c* oxidase subunit IV (COXIV), as well as by the high level of peroxisomal Catalase (Fig. 1 A). Similar amounts of UQ$_9$ were detected in the fractions from both genotypes (Fig. 1 D), whereas UQ$_{10}$ was undetectable (not depicted).

We also determined the UQ content in plasma membrane fractions whose purity and enrichment were assessed by using Pan-Cadherin as a specific plasma membrane marker (Fig. 1 E). No differences in UQ$_9$ or UQ$_{10}$ content were observed between the two genotypes (Fig. 1 F).

The UQ distribution within mitochondria is altered in *Mclk1*$^{+/-}$ mutants

An additional approach based on submitochondrial fractionation was used to quantify UQ$_9$ and UQ$_{10}$ in individual mitochondrial membranes as well as in the soluble fraction. Specific protein markers were used for each mitochondrial compartment to verify enrichment, purity, and determine potential differences between genotypes (Fig. 2 A). The Western blot results confirm that specific fractions were successfully obtained for all compartments and that markers are expressed similarly in *Mclk1*$^{+/+}$ and *Mclk1*$^{+/-}$ mitochondria. Indeed, monoamine oxidase (MAO) expression was only detected in the outer membrane (OM) fraction, and COXIV was strongly expressed in the inner membrane (IM) fraction, with only traces in the OM, whereas the second mitochondria-derived activator of caspases (SMAC) was mainly detected in the soluble fraction, as expected (Fig. 2 A). Quantification of UQ in these fractions revealed significantly elevated UQ$_9$ and UQ$_{10}$ in the OM of *Mclk1*$^{+/-}$ mutants compared with control littermates (Fig. 2 B and Fig. S1). In contrast, the UQ$_9$ content of the IM of *Mclk1*$^{+/-}$ mutants was significantly decreased in comparison to *Mclk1*$^{+/+}$ control littermates (Fig. 2 C). Consequently, the OM/IM ratio for UQ$_9$ content is significantly different between genotypes (Fig. 2 D). A trend toward a decrease was also observed for UQ$_{10}$ in the same fractions, but the difference didn't reach significance (Fig. S1). In the soluble fraction, which includes components of the inter-membrane and matrix compartments, little UQ$_9$ was detected and no difference between genotypes was observed (Fig. 2 E). No UQ$_{10}$ was detected in the soluble fractions (unpublished data).

Our observations suggest that in *Mclk1*$^{+/-}$ mutants there is more UQ in the OM and less UQ in the IM than in the wild type. To confirm that protein compositions of both mitochondrial membranes were not affected by reduced MCLK1 levels,

we quantified additional proteins specific to the OM and the IM in relation to the level of a protein of the soluble fraction (CypD) in pairs of siblings of the two genotypes (Fig. 3 A). We found that the $Mclk1^{+/-}$ genotype had no impact on individual protein levels. This suggests that the integrity and balance of the mitochondrial proteome is not affected in $Mclk1^{+/-}$ mitochondria. This further suggests that the ratio of lipids to protein is unaltered in these membranes. In addition, the ultrastructure of liver mitochondria was examined by transmission electron microscopy. It revealed morphologically normal mitochondria in $Mclk1^{+/-}$ mutants. Mutant mitochondria were indistinguishable from the wild type in size and shape. Both IMs and OMs were intact and the space between them was as in the wild type. Finally, no obvious abnormalities were observed in the number and shape of cristae (Fig. 3 B). We conclude that the UQ deficiency in the IM is a direct consequence of low UQ synthesis in the IM.

Functional significance of changes in UQ distribution

The lower level of UQ in the IM could be the cause of several reported $Mclk1^{+/-}$ mice phenotypes, including: (a) the decline in electron transport between complex I and III as well as between complex II and III; (b) the decreased oxygen consumption of isolated mitochondria with complex I or complex II substrates; and (c) the reduction in mitochondrial ATP levels (Lapointe and Hekimi, 2008; Lapointe et al., 2009). The electron carrier function of UQ from complex I and II to complex III is the most well-established function of UQ, as is the relation between the electron transport rate and UQ concentration (Schneider et al., 1982). It has been reported that endogenous UQ levels are not saturating for NADH oxidation by complex I and, possibly, for succinate oxidation by complex II (Norling et al., 1974; Lenaz et al., 1997). This suggests that variations in physiological UQ levels should impact electron transport in the mitochondrial respiratory chain (Fato et al., 1997). Although UQ is present in mitochondria at a much higher concentration than other constituents of the ETC, it is believed that lowering UQ levels could affect mitochondrial function because of its slow rate of oxidation reduction, whether or not the traditional random collision mechanism or the more recent model involving supercomplex organization is considered (Green and Tzagoloff, 1966; Lenaz and Genova, 2009). Together, these observations suggest that the reduction in MCLK1 levels in $Mclk1^{+/-}$ mutants leads to a reduction of the UQ content of the IM, which falls below that required for maintaining physiologically normal levels of electron transport.

The UQ deficiency in the IM could also be the cause of the oxidative stress observed in $Mclk1^{+/-}$ mitochondria. The mitochondrial ETC is believed to be a major site of cellular ROS production, and lower respiratory rates resulting from inhibition of electron transport are often accompanied by enhanced ROS release. Moreover, respiratory dysfunction and oxidative stress resulting from UQ deficiency have been reported in various experimental conditions and specific pathologies (Geromel et al., 2002; DiMauro et al., 2007). For example, human skin fibroblasts carrying a homozygous mutation in the $COQ2$ gene,
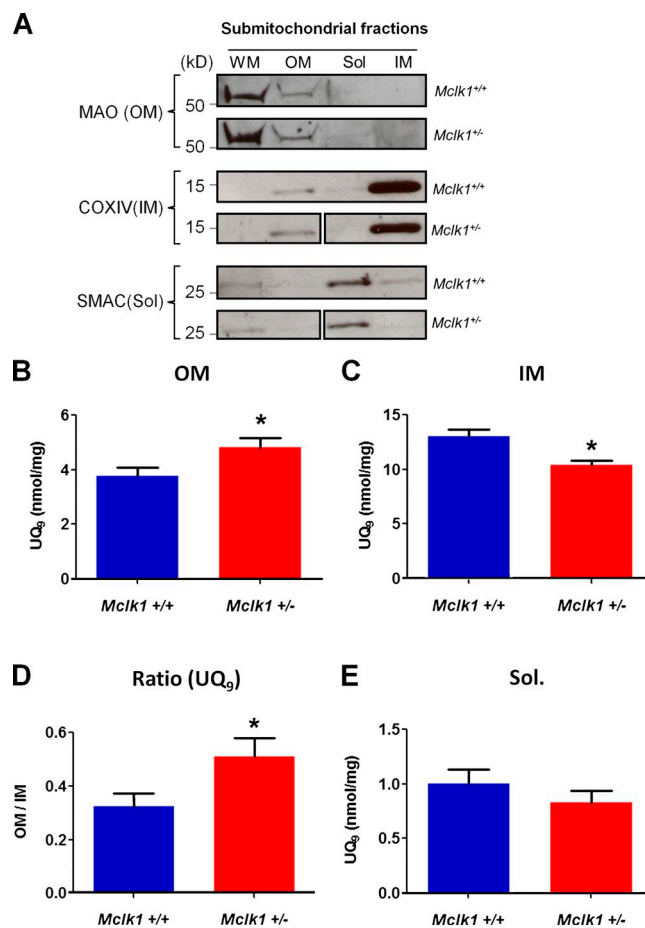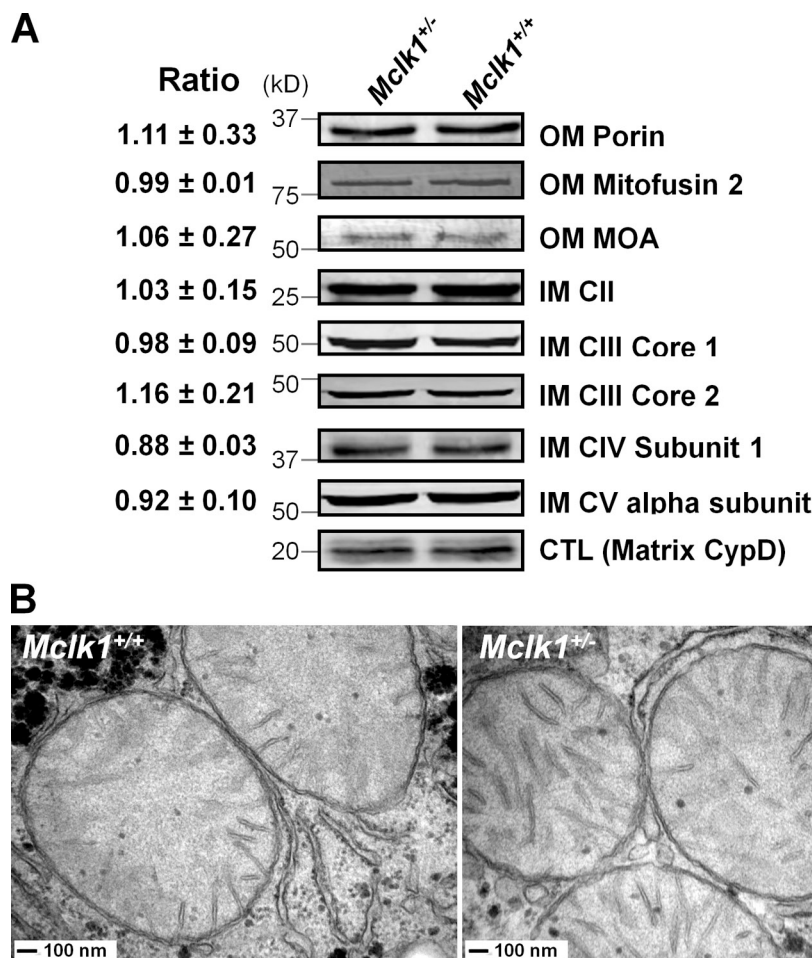

Figure 2. **Unique intramitochondrial distribution of UQ in $Mclk1^{+/-}$ mice.** (A) Mitochondrial markers were used to assess the purity of each fraction generated as described in the main text: whole mitochondria (WM), OM, soluble fraction (Sol), and IM. Monoamine oxidase (MAO) was used as marker for the OM fraction, COXIV for the IM fraction, and SMAC for the soluble fraction (Sol). For each antibody, the samples were analyzed on separate Western blots; all samples for both genotypes were run on a single gel, one gel for each Western blot. For presentation purposes the third and fourth lane for the $Mclk1^{+/-}$ samples (to the right of the white line) for the COXIV and SMAC Westerns have been switched relative to the order in the original gel. Note that COXIV was easily detected in the WM fraction with longer exposure (not depicted). The positions of selected molecular mass markers in the original blots are indicated in kilodaltons (kD). (B) Significantly more UQ_9 was found in the OM fraction of $Mclk1^{+/-}$ mice. (C) Significantly less UQ_9 was found in the IM fraction of $Mclk1^{+/-}$ mice. (D) The evaluation of the UQ_9 ratio (OM/IM) shows the different UQ distribution within $Mclk1^{+/-}$ mitochondria. (E) UQ_9 in the soluble fraction was low and not different between genotypes. UQ_{10} was undetectable. Data are the means ± SEM of 10–15 mice (error bars). The asterisk denotes significance at P < 0.05.

which encodes a protein implicated in the UQ biogenesis pathway, have significantly less cellular UQ and exhibit a mitochondrial phenotype highly similar to that of $Mclk1^{+/-}$ mice (López-Martin et al., 2007). In these fibroblasts, UQ deficiency is also linked to a partial defect in electron transport and ATP synthesis, as well as significantly increased ROS production and oxidation of lipids and proteins (López-Martin et al., 2007; Quinzii et al., 2008, 2010).

The increase in UQ levels in the OM is an unexpected outcome of the partial loss of a UQ biosynthetic enzyme. One possibility is that this phenotype is linked to the antioxidant

Figure 3. **Mitochondrial membrane protein composition and ultrastructure are not affected in *Mclk1+/−* mice.** (A) Representative Western blots and relative amounts (Ratio) show comparable amounts in the two genotypes. Equal amounts of total protein (20 µg) were loaded for all samples, and the matrix protein Cyclophilin D (CypD) was used as control to correct for minor variations in loading. The ratio values are presented as relative abundance of each protein normalized to CypD. Data are the means ± SEM of 4 mice. The positions of selected molecular mass markers in the original blots are indicated in kilodaltons (kD). OM proteins: Mitofusion 2, monoamine oxidase A (MOA), and Porin. IM proteins: Complex II (CII), Complex III–Core protein 1 (CIII Core 1), Complex III–Core protein 2 (CIII Core 2), CIV Subunit 1, and CV α subunit. Matrix protein CypD was used as a loading control. (B) Transmission electron microscopy images of liver mitochondria. Magnification is 30,000 and representative of *n* = 2 animals per genotype.

Ratio	(kD)	Mclk1+/−	Mclk1+/+	
1.11 ± 0.33	37			OM Porin
0.99 ± 0.01	75			OM Mitofusin 2
1.06 ± 0.27	50			OM MOA
1.03 ± 0.15	25			IM CII
0.98 ± 0.09	50			IM CIII Core 1
1.16 ± 0.21	50			IM CIII Core 2
0.88 ± 0.03	37			IM CIV Subunit 1
0.92 ± 0.10	50			IM CV alpha subunit
	20			CTL (Matrix CypD)

Mclk1+/+ — 100 nm   *Mclk1+/−* — 100 nm

functions of UQ. As discussed above, it is likely that the low level of UQ in the IM of *Mclk1+/−* mutants increases oxidative stress by partially inhibiting electron transport. It is well known that under oxidative stress, cells will take protective measures to ensure their survival, such as increasing the levels of an antioxidant such as UQ. In fact, overall tissue levels of UQ have been found to be elevated by conditions that increase oxidative stress and damage (Guan et al., 1996; Navarro et al., 1998). Thus elevation of UQ levels in the OM of *Mclk1+/−* mutants might be a protective response to reduce oxidative damage to the OM and/or reduce ROS leakage from the mitochondria to the cytoplasm. The mechanism by which the mitochondria increase UQ levels in the OM is unknown but could be based on slower turnover or slower export of UQ.

Reduction of COQ3 levels in *Coq3+/−* heterozygotes does not result in a *Mclk1+/−*-like phenotype

We wondered whether the appearance of a mitochondrial UQ imbalance in heterozygotes is specific to the *Mclk1* locus or is a more general characteristic of genes that code for UQ biosynthetic enzymes, which, at least in yeast, function in a supramolecular complex (Turunen et al., 2004). We thus created a targeted inactivation of the mouse *Coq3* gene. No *Coq3* homozygous mice were obtained from heterozygous crosses,

indicating that *Coq3* is essential for embryonic survival. Of 211 live pups from heterozygous mating, 83 were wild type and 128 were hemizygous. This ratio is close to the 1:2 ratio typical for an embryonic lethal gene. As expected, we observed that *Coq3* transcription is decreased in *Coq3+/−* heterozygotes (Fig. 4 A). We raised an antiserum against mouse COQ3 and could show that *Coq3+/−* mice display low COQ3 protein levels (Fig. 4, B and C). Similarly to *Mclk1+/−*, no changes in UQ levels were observed in pure mitochondria isolated from 3-mo-old *Coq3+/−* livers (Fig. 4 D). However, submitochondrial fractionation did not reveal any significant difference in UQ content within mitochondrial compartments (Fig. 4, E and F). As expected from the above results, mitochondrial function assessed by in vitro oxygen consumption experiments as well as mitochondrial oxidative status, which was analyzed by measuring aconitase activity, were not affected by the reduced COQ3 levels (Fig. S2, A and B). Finally, we examined the age-dependent survival of both male and female *Coq3+/−* mice and found that both sexes exhibited normal life spans (Fig. S2, C and D). These results indicate that COQ3, in contrast to MCLK1, is not limiting for UQ biosynthesis, in spite of acting twice in the UQ biosynthetic pathway. This observation does not support the idea that the complex UQ phenotype of *Mclk1+/−* mice is related to a supramolecular complex of UQ biosynthetic enzymes.

Supplemented dietary UQ_{10} induces changes in intramitochondrial UQ distribution

UQ level increases resulting from dietary UQ supplementation have been found to be greater in mitochondria than in whole tissue homogenates (Kamzalov et al., 2003; Fernández-Ayala et al., 2005; Saito et al., 2009), and orally supplemented UQ is able to restore mitochondrial dysfunction and decrease oxidative damage resulting from UQ deficiency (Geromel et al., 2002; López et al., 2010; Dai et al., 2011). Surprisingly, in spite of this, nothing appears to be known about the intramitochondrial fate of exogenous UQ.

To evaluate the cellular fate of exogenous UQ_{10}, we used a formulation (Q-Gel from Tishcon) that results in consistent UQ uptake (Kamzalov et al., 2003; Preuss et al., 2010). Significant accumulation of UQ_{10} was detected in whole liver and liver mitochondria of UQ_{10}-supplemented mice (Fig. S3, A and C). Interestingly, we observed a greater accumulation of UQ_{10} in both $Mclk1^{+/-}$ livers (Fig. S3 A), and purified $Mclk1^{+/-}$ liver mitochondria, where the trend was significant; that is, $Mclk1^{+/-}$ mitochondria accumulated more exogenous UQ_{10} than their $Mclk1^{+/+}$ counterparts (Fig. S3 C). It is thought that UQ uptake by tissues could be enhanced if the endogenous UQ levels have fallen below a critical threshold (Sohal and Forster, 2007). The effect could also be the result of a reaction to the greater oxidative stress due to the intrinsic UQ_9 IM deficiency. However, endogenous total UQ_9 levels were not affected by UQ_{10} treatment (Fig. S3, B and D).

Supplemented UQ_{10} was also followed in submitochondrial fractions. We report here, for the first time to our knowledge, that exogenous UQ_{10} is successfully incorporated in both the OM and the IM (Fig. 5, A and C). Although we observed increased UQ_{10} incorporation in whole $Mclk1^{+/-}$ mitochondria (Fig. S3 C), this was not observed when membranes preparations were used (Fig. 5, A and C). Possibly, some of the exogenous UQ is more loosely bound to membranes than endogenous UQ and is lost during membrane preparation.

We further observed that UQ_{10} supplementation reduced UQ_9 content in the OM of $Mclk1^{+/-}$ mutants to wild-type levels (Fig. 5 B). It is possible that the antioxidant properties of the exogenous UQ_{10} decreased the need for more UQ_9 in the $Mclk1^{+/-}$ OM, and/or saturating concentrations for UQ of any side-chain length are being generated in the OM by the UQ_{10} supplementation (Kwong et al., 2002). However, a UQ_9 deficit was still observed in the $Mclk1^{+/-}$ IM after UQ_{10} administration, and this even while UQ_{10} content was dramatically increased (Fig. 5, C and D). Orally supplemented UQ_{10} has been shown to increase tissue concentrations of endogenous UQ_9 by an unknown mechanism, but this was obtained with a much longer duration of treatment (Kamzalov et al., 2003).

Rescue of $Mclk1^{+/-}$ mitochondrial defects by exogenous UQ

Rescue of $Mclk1^{+/-}$ mitochondrial defects in vitro was not attempted previously because no UQ deficiency had been observed. The activity of complex II is measured by following the decrease in absorbance caused by the coupled reduction
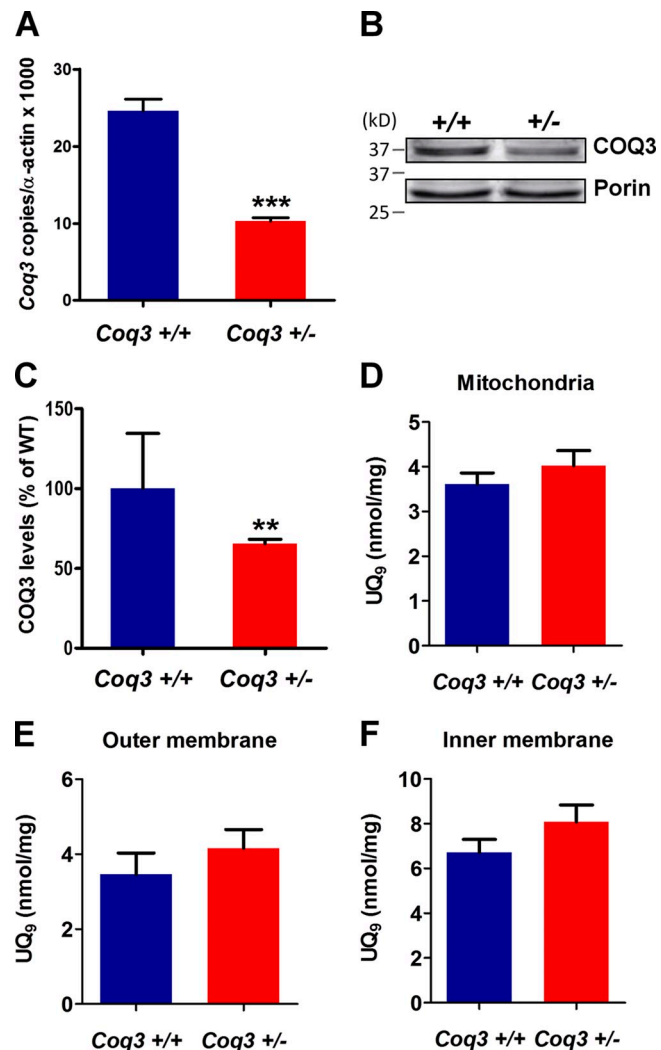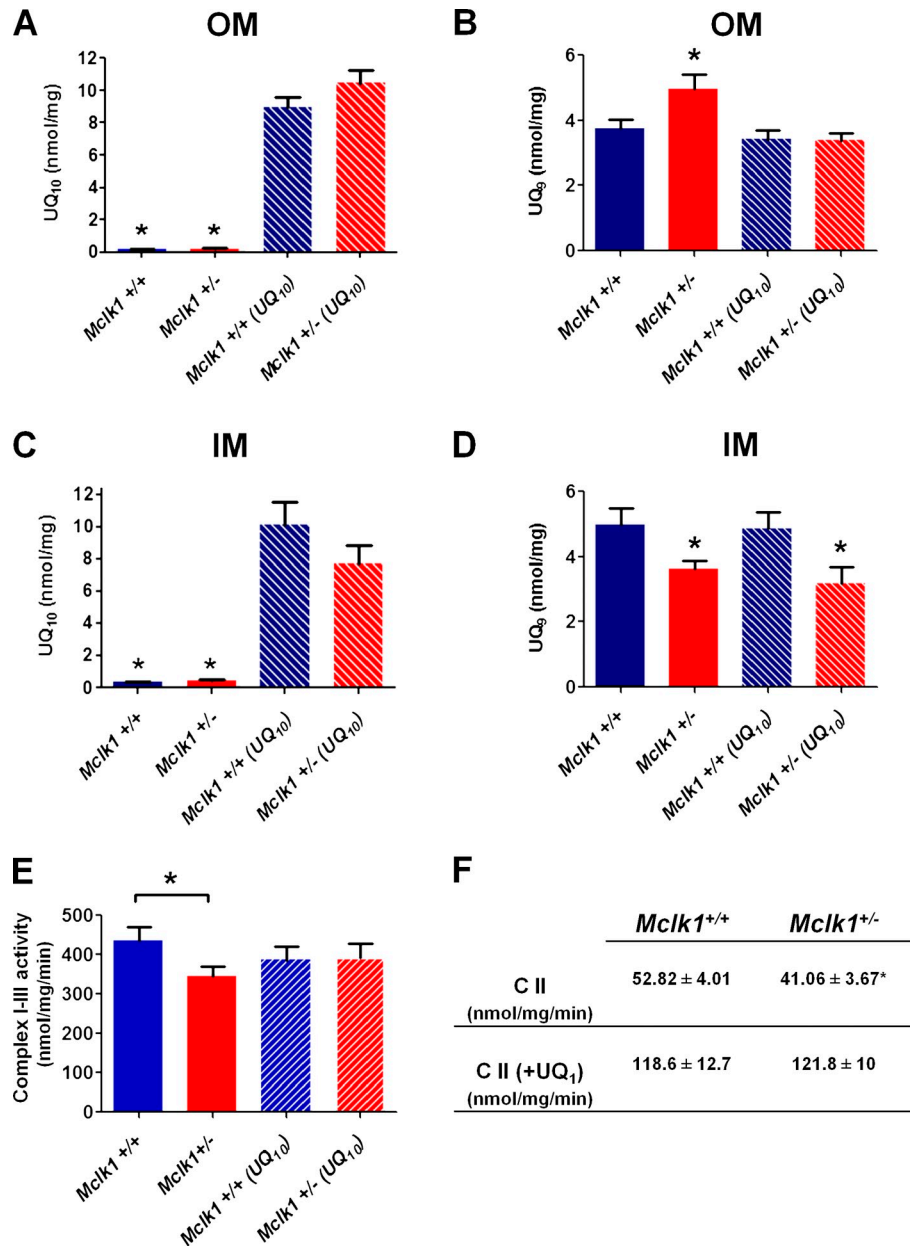
Figure 4. **The phenotype of $Coq3^{+/-}$ mice.** (A) $Coq3$ mRNA levels in liver of $Coq3^{+/-}$ and $Coq3^{+/+}$ littermate by RT-PCR. (B) Representative Western blots showing COQ3 and Porin levels in mitochondria from liver. The positions of selected molecular mass markers in the original blots are indicated in kilodaltons (kD). (C) Band intensities are presented as the percentage of COQ3 to Porin ratio of the $Coq3^{+/+}$ mice. (D) No difference in UQ_9 in liver mitochondria of the two genotypes was observed. (E and F) No differences in UQ_9 were found in the OM and IM of $Coq3^{+/+}$ and $Coq3^{+/-}$ mice after submitochondrial fractionation. Data are the means ± SEM of 5 mice for COQ3 mRNA and protein quantification and of 8–15 mice for UQ quantification. The asterisks denote statistical significance of the difference between $Mclk1^{+/+}$ and $Mclk1^{+/-}$ animals at P < 0.01 (**) and P < 0.001 (***).

of 2,6-dichlorophenolindophenol at 600 nm with 750 nm as the reference wavelength (see Materials and methods). Under these native conditions, there is a clear decrease in mutant complex II activity in mitochondria isolated from both liver and kidneys (Fig. 5 F and Fig. S3 E). However, no difference in complex II activity between the wild type and $Mclk1^{+/-}$ mutants could be observed when exogenous UQ_1 was added to the reaction (Fig. 5 F and S3 E). This suggests that the reduction in endogenous UQ_9 in the IM is sufficiently severe to impact ETC functions, in this case electron transport from complex II to UQ.

Figure 5. Effects of supplemented dietary UQ$_{10}$ on intramitochondrial UQ distribution and electron transport in *Mclk1*$^{+/-}$ mice. (A) Supplemented dietary UQ$_{10}$ accumulated in the OM fractions of treated animals (*Mclk1*$^{+/+}$ [UQ$_{10}$] and *Mclk1*$^{+/-}$ [UQ$_{10}$]). (B) Significantly more UQ$_9$ was detected in the *Mclk1*$^{+/-}$ OM, but this difference was abolished by UQ$_{10}$ supplementation (*Mclk1*$^{+/-}$ [UQ$_{10}$]). (C) Supplemented UQ$_{10}$ accumulated in the IM of treated animals (*Mclk1*$^{+/+}$ [UQ$_{10}$] and *Mclk1*$^{+/-}$ [UQ$_{10}$]). (D) The IM of *Mclk1*$^{+/-}$ mutants contains significantly less UQ$_9$ than that of their *Mclk1*$^{+/+}$ littermates, and this was not affected by UQ$_{10}$ supplementation (*Mclk1*$^{+/-}$ [UQ$_{10}$]). (E) Electron transfer between complex I and III was measured in treated and untreated mice of both genotypes. A significant decrease in complex I–III activity in *Mclk1*$^{+/-}$ mice compared with control *Mclk1*$^{+/+}$ mice was observed as previously reported (Lapointe and Hekimi, 2008). This electron transport dysfunction was not observed anymore after UQ$_{10}$ supplementation (no difference between *Mclk1*$^{+/+}$ [UQ$_{10}$] and *Mclk1*$^{+/-}$ [UQ$_{10}$] mice). (F) Complex II is affected in liver mitochondria of *Mclk1*$^{+/-}$ mice (as reported in Lapointe and Hekimi, 2008). However, this defect in electron transport is suppressed when soluble UQ$_1$ is provided. Data are the means ± SEM of 8–15 mice (error bars). The asterisk denotes significance at P < 0.05.

A OM — UQ$_{10}$ (nmol/mg)

B OM — UQ$_9$ (nmol/mg)

C IM — UQ$_{10}$ (nmol/mg)

D IM — UQ$_9$ (nmol/mg)

E Complex I-III activity (nmol/mg/min)

Categories: Mclk1 +/+, Mclk1 +/-, Mclk1 +/+ (UQ$_{10}$), Mclk1 +/- (UQ$_{10}$)

F

	Mclk1$^{+/+}$	*Mclk1*$^{+/-}$
C II (nmol/mg/min)	52.82 ± 4.01	41.06 ± 3.67*
C II (+UQ$_1$) (nmol/mg/min)	118.6 ± 12.7	121.8 ± 10

Exogenous supplemented UQ$_{10}$ is able to increase mitochondrial electron transport in either normal or UQ-deficient conditions (Fernández-Ayala et al., 2005; López-Martin et al., 2007). A recent publication also suggests that UQ$_{10}$ supplementation might restore several of the phenotypes of *C. elegans* *clk-1* mutants (Takahashi et al., 2012). To assess whether the accumulation of supplemented UQ$_{10}$ in the IM is functional, we tested whether it could rescue one of the reported electron transport chain dysfunction of the *Mclk1*$^{+/-}$ mice. We analyzed electron transport between mitochondrial complex I and III, a defect that can reasonably be attributed to the UQ$_9$ deficiency observed in the *Mclk1*$^{+/-}$ mitochondrial IM. Although, as expected, a clear difference between *Mclk1*$^{+/+}$ and *Mclk1*$^{+/-}$ mice was observed in the control mice, electron transport rates in the two genotypes were indistinguishable after UQ$_{10}$ treatment (Fig. 5 E). The rate of electron transport in the wild-type UQ$_{10}$-treated mice appeared somewhat lower than in untreated wild-type mice, but the difference was not significant. This result suggests that the exogenous UQ$_{10}$ was indeed capable of rescuing the endogenous UQ$_9$ deficiency. Although it is possible in principle that the UQ$_{10}$ specifically depressed the rate in the wild type but was without effect in the mutant, this appears unlikely.

The findings presented here, that there is an IM-specific UQ deficiency in *Mclk1*$^{+/-}$ mutants and that at least some of the mitochondrial phenotypes of these mutants can be rescued in vitro and in vivo by exogenous UQ, should prompt further study to determine if all *Mclk1*$^{+/-}$ phenotypes can be rescued by exogenous UQ, including whole animal phenotypes such as aging, immune activation, and resistance to cerebral ischemia/reperfusion injury (Liu et al., 2005; Wang et al., 2010; Zheng et al., 2010).

Conclusions

Our study lays emphasis on the importance of carefully analyzing individual mitochondrial compartments when studying membrane-associated mitochondrial proteins or lipids. This approach has helped us to reveal that MCLK1 activity is limiting for normal UQ content in the mitochondrial IM and that in turn UQ content in this membrane is a limiting factor for electron transport chain activity. In the light of our findings, we also propose that the distribution of UQ in mitochondrial membranes is likely to be an adaptive and dynamic process that can react to changes in UQ synthesis or absorption. Our demonstration that exogenous UQ is able to successfully reach the inner mitochondrial membrane is also important when UQ is used or studied for therapeutic purposes.

Materials and methods

Animals

All the animals were housed in a pathogen-free facility at McGill University and were given a standard rodent diet and water ad libitum. $Mclk1^{+/+}$ and $Mclk1^{+/-}$ mice, 3-mo-old males and females from pure BALB/c genetic background, were anesthetized, sacrificed by cervical dislocation, and perfused with phosphate buffer. Tissues were then rapidly removed, rinsed, and placed in ice-cold mitochondrial isolation buffer or immediately frozen in liquid nitrogen. All procedures were approved by the McGill Animal Care and Ethics committees.

Generation of *Coq3* gene knockout mice

Coq3 gene knockout mice were generated by inGenious Targeting Laboratories, Inc., using bacterial artificial chromosome (BAC)-mediated recombination. In brief, a mouse genomic *Coq3* fragment with 10.1 kb of upstream homology sequence and 2.1 kb of downstream homology sequences was subcloned into a targeting vector. A loxP/FRT-flanked PGK-neomycin resistance cassette was then inserted to replace exons 4 and 5 of the *Coq3* gene. NotI-linearized targeting vector was transfected into 129SV/EV embryonic stem cells. Clones were selected in G418, and PCR analysis identified clones that had undergone homologous recombination were microinjected into 129/SvEv blastocysts. The resulting chimeric mice were mated with 129/SvEv mice to generate heterozygous germ-line founders. *Coq3* heterozygous mice appear normal and fertile, whereas *Coq3*-null mice die in utero. For PCR genotyping, DNA was extracted from tail clippings and subjected to PCR using the following primers: KO (5′-GGGGAACTTC-CTGACTAGGG-3′) and GR (5′-CGAGGATTGAGGGTCAGGTA-3′) to identify the disrupted allele (522 bp) and wild type (5′-CCAGTGCTGC-TATCAAGTGC-3′) and GR to identify the wild-type allele (345 bp). PCR conditions were 94°C for 3 min, 94°C for 30 s, 56°C for 30 s, and 72°C for 1 min for 30 cycles followed by 72°C for 10 min. PCR products were resolved on 2% agarose gels.

Isolation of pure mitochondrial fractions

On the day of the experiment, fresh liver was homogenized in 10 vol (wt/vol) of MSHE buffer (210 mM Mannitol, 75 mM sucrose, 10 mM Hepes, pH 7.2, and 1 mM EGTA). The resultant homogenate was centrifuged at 600 g for 10 min at 4°C in an Allegra X-12 bench-top centrifuge (Beckman Coulter) to remove large cellular debris. The 600 g supernatant was centrifuged at 15,000 g for 10 min, and the mitochondria-enriched pellet was further washed with MSHE and centrifuged again at 15,000 g for 10 min in an Avanti J-25 centrifuge (Beckman Coulter). The supernatant corresponded to the cytosolic fraction. The washed pellet was then resuspended in 2 ml of 35% Histodenz (Sigma-Aldrich) prepared in MSHE for further purification using ultracentrifugation through a discontinuous Histodenz gradient (15%, 25%, 35%, and 40%; Graham, 1993). The resuspended pellet obtained was carefully layered on top of 2 ml of 40% Histodenz, and this was topped off with 1 ml of 25% and finally 1 ml of 15% Histodenz. The sealed tubes were centrifuged for 90 min at 52,000 g at 4°C in an Optima MAX ultracentrifuge (Beckman Coulter). The predicted bands of particles seen after such centrifugation with those specific Histodenz solutions are: peroxisomes at the 35/40% interface (Graham, 2001b), mitochondria at the 25/35% interface (Graham, 2001c), and lysosomes at the 15/25% interface (Graham, 2001a; Okado-Matsumoto and Fridovich, 2001).

The band at the 25/35% interface, which contained mitochondria, was collected, diluted in MSHE buffer, and centrifuged at 10,000 g_{max} to pellet mitochondria. The isolated mitochondria were resuspended again in 35% Histodenz and submitted to a second Histodenz density-gradient purification following the same procedure. The purity of the mitochondrial preparations obtained after this procedure was further verified by classical immunoblot experiments with antisera against mitochondrial Porin (EMD Millipore) and mitochondrial COXIV (New England Biolabs, Inc.). The presence of contaminating peroxisomes was checked with a specific antibody against peroxisomal enzyme Catalase (EMD Millipore).

Isolation of pure peroxisomal fractions

Peroxisomes were purified by density gradient using Histodenz medium (Sigma-Aldrich) as described previously (Graham, 2001b), with some modifications. In brief, liver was first processed exactly as it was described earlier for mitochondrial isolation, except that the band at the 35/40% interface, corresponding to the fraction enriched in peroxisomes (Graham, 2001b), was collected and diluted with the same volume of MSHE buffer and then centrifuged at 15,000 g for 10 min. The pellet obtained was resuspended in 2 ml of 35% Histodenz before further purification on Histodenz gradient. This gradient was prepared by carefully topping the resuspended peroxisomes (in 35% Histodenz) with 2 ml of 25% and 1.5 ml of 15% Histodenz solutions, and centrifuged at 52,000 g for 60 min at 4°C. The purified peroxisomes were then recovered from the pellet, diluted in an equal volume of MSHE buffer, centrifuged at 15,000 g for 10 min, and resuspended again in 35% Histodenz for a second round of purification. Then, the peroxisomal pellet was resuspended in MSHE for immunoblots and HPLC analysis. Fraction purity and possible mitochondrial contamination was assayed via immunoblots analysis of specific markers (peroxisomes, anti-Catalase [EMD Millipore]; mitochondria, anti-Porin [EMD Millipore] and anti-COXIV from New England Biolabs, Inc.).

Isolation of plasma membrane fraction

Plasma membrane fractions were purified according to a published protocol (Song et al., 2006). Mouse livers were homogenized in 10 vol (wt/vol) of MSHE buffer with a Potter homogenizer (Teflon pestle). The homogenates were then centrifuged for 10 min at 1,000 g at 4°C. The pellet was suspended in 20 ml of buffer A (0.3 M sucrose, 50 mM Tris, and 3 mM $MgCl_2$, pH 7.5) and mixed with 9 volumes of buffer B (1.98 M sucrose, 50 mM Tris, and 1 mM $MgCl_2$, pH 7.5) to form 1.8 M (50% wt/wt) sucrose density. After centrifugation at 70,900 g for 90 min, the 0.25 M/1.8 M interface (8.3/50% sucrose) was collected and resuspended in 0.25 M SHE (0.25 M sucrose, 10 mM Hepes, pH 7.5, and 1 mM EDTA). The suspension was centrifuged at 1,200 g for 10 min, and the resulting pellet was resuspended using 0.25 M SHE. 2.4 M SHE (2.4 M sucrose, 10 mM Hepes, pH 7.5, and 1 mM EDTA) was added to bring the final concentration to 1.45 M. The suspended pellet was then overlaid with 0.25 M SHE to fill the tubes and centrifuged at 68,400 g for 60 min. The pellet was resuspended in 0.25 M SHE, mixed with 2.4 M SHE to bring the final concentration of sucrose to 1.35 M, and centrifuged at 230,000 g for 60 min. The material at the 0.25 M/1.35 M interface (8.3/39% sucrose) was collected and constituted the plasma-membrane fraction. Enrichment and specificity of the plasma membrane fractions were assayed by immunoblots analysis of specific markers anti–Pan-cadherin (Sigma-Aldrich) and anti-Porin (EMD Millipore).

Mitochondrial subfractionation

The purified mitochondria were recovered from the 25/35% interface of the Histodenz gradient as described earlier, diluted in an equal volume of MSHE buffer, centrifuged at 15,000 g for 10 min, and resuspended in MSHE. The separation of inner and outer mitochondrial membranes was performed by resuspending the gradient-purified mitochondria in 0.75% digitonin in isolation medium (220 mM Mannitol, 70 mM sucrose, 20 mM Hepes-NaOH, pH 7.4, and 0.5 mg/ml fatty-acid-free bovine serum albumin) on ice for 20 min with gentle agitation as described previously (Graham, 1993). The resulting mitochondrial suspension was then diluted with 3 vol of isolation medium, mixed carefully by three strokes in a loose fitting Dounce homogenizer, and gently sonicated two times for 15 s at 40 W. Mitoplasts (IM and matrix) were separated from the supernatant (OM and the inter membrane space content) by centrifugation at 15,000 g for 15 min. The OM fraction was obtained by centrifugation of the supernatant at 100,000 g for 60 min. The resulting pellet was resuspended in pure water and centrifuged again at 15,000 g for 15 min. The pellet was resuspended in pure water and sonicated eight times for 15 s at 80 W with 15 s of rest. The IM and matrix fractions were then separated by

centrifugation at 200,000 g for 45 min. OM and IM fractions were resuspended in MSHE buffer. Fraction purity was assayed by immunoblot analysis of specific fractions markers (OM, anti-monoamine oxidase [Santa Cruz Biotechnology, Inc.]; IM, anti-COXIV (EMD Millipore); soluble fraction, anti-SOD2 (Cedarlane) and anti-SMAC (EMD Millipore) as described previously (Da Cruz et al., 2003). All the fractions were frozen at –80°C for subsequent immunoblot and HPLC analysis.

Relative quantification of mitochondrial membrane proteins
Mitochondria were isolated from the livers of 3-mo-old $Mclk1^{+/-}$ mutant and wild-type sibling mice. 20 µg of mitochondrial protein/sample was subjected to Western blot analysis with antibodies against the following proteins: Mitofusion 2, monoamine oxidase A (MOA), and Porin in the OM; respiratory complexes II–V in the IM; and Cyclophilin D located in the matrix of mitochondria. All antibodies were obtained from Abcam. Blots were visualized using ECL plus Western blotting detection system (GE Healthcare) with a Typhoon 9400 scanner (GE Healthcare). Band intensities were analyzed using ImageJ software and normalized to those of Cyclophilin D.

Electron microscopy
3-mo-old mice on the BALB/c genetic background were anesthetized and subjected to intracardiac perfusion with Ringer's lactate solution and 2.5% glutaraldehyde in 0.1 M sodium cacodylate buffer and 4% sucrose. Livers were removed, cut into small pieces, and immersed in the same fixative overnight at 4°C. After washing with 0.1 M cacodylate buffer, pH 7.4, the sample specimens were postfixed in 1% OsO4 and 1.5% potassium ferrocyanide for 2 h and then routinely processed for transmission electron microscopic observation. In brief, the postfixed specimens were dehydrated through a series of graded acetone solutions, infiltrated with epon-acetone mixture, and embedded in epon. Polymerization was performed at 60°C for 2 d. Ultrathin sections (90–100 nm) were then mounted on copper grids and counterstained with uranyl acetate and Reynold's lead citrate. Observations were performed on a Tecnai 12 BioTwin Transmission Electron Microscope (FEI Electron Optics), operated at 120 kV, using a 40-µm objective aperture. Images were digitized with the use of an AMT XR80C (8 megapixel) charge-coupled device camera and Image Capture Engine Software (version 601).

Two animals were analyzed per group. At least three randomly selected sections from each animal were visualized by transmission electron microscopy for mitochondrial morphological integrity. In each section, >20 random selected mitochondria from different fields of view were examined.

Identification of quinones
Cellular fractions or submitochondrial fractions were mixed with an equal volume of 100% ethanol (Thermo Fisher Scientific) and vortexed for 10 s. An equal volume of hexane (Sigma-Aldrich) was then added followed by 2 min of vortexing and 5 min of centrifugation (8,000 g, 4°C).The resulting upper layer was collected and evaporated to dryness using a Speed Vac (Eppendorf Concentrator), after which the residual was resuspended in 100% ethanol and stored at −20°C until HPLC analysis. A Beckman System Gold HPLC with a reversed-phase C18 column (5 µm, 4.6 × 250 mm) was used. The mobile phase was 70% methanol and 30% ethanol at a flow rate of 1.8 ml/min. The UV detector was set at 275 nm. Quinones were identified and quantified using pure UQ standards from Sigma-Aldrich. The total amount of quinone was normalized to the amount of protein (Liu et al., 2005).

Determination of Coq3 mRNA and protein expression
Livers harvested from 3-mo-old female wild-type and $Coq3^{+/-}$ mice were quick-frozen in liquid nitrogen and stored at −80°C until use. Quantitative real-time PCR was used to determine the mRNA expression level of $Coq3$ in liver using the following primers for Coq3 and the housekeeping gene β-actin: Coq3-F, 5′-ACGGGTGCCATTCATTAGAG-3′; Coq3-R, 5′-TGAAGCTCCCAGTCTCCCTA-3′; β-actin-F, 5′-CACACCCGCCACCAGTTCGC-3′; and β-actin-R, 5′-CCACCATCACACCCTGGTGCC-3′. Standard curves for each primer set were generated using a dilution series of known amounts of purified PCR products. The $Coq3$ mRNA levels were normalized to the amount of β-actin mRNA in the same samples, and the final real-time RT-PCR results are reported as copy number of $Coq3$ per 1,000 copies of β-actin. Quantitative real-time PCR was performed using SYBR-Green PCR Master Mix on a CFX96 real-time PCR instrument (Bio-Rad Laboratories), according to the manufacturer's instructions. The level of COQ3 protein was determined by Western blot analysis with an anti-COQ3 antibody

(developed in our laboratory). In brief, 18 µg of mitochondrial protein samples were electrophoresed on 12% SDS-polyacrylamide gels and transferred to polyvinylidene fluoride (PVDF) membrane (Bio-Rad Laboratories). The membranes were probed first with rabbit polyclonal anti-COQ3 (dilution 1:1,000) and anti-Porin (dilution 1:1,000; Abcam) antibodies overnight, followed by peroxidase-conjugated secondary anti-rabbit antibody (dilution 1:2,000; Sigma-Aldrich). The blots were developed using ECL-Plus kit (GE Healthcare) and visualized with a Typhoon 9400 scanner (GE Healthcare).

Oxygen consumption by isolated mitochondria
Oxygen consumption was measured polarographically as described by Lapointe and Hekimi (2008). In brief, liver mitochondria were prepared from freshly sacrificed 3-mo-old female mice using Mg^{2+}-free buffer containing 0.25 M sucrose, 10 mM Hepes, pH 7.4, and 1 mM EDTA. Oxygen consumption was measured in the air-saturated respiration buffer (250 mM sucrose, 10 mM Hepes, pH 7.2, 20 mM KCl, 5 mM KH$_2$PO$_4$, and 2 mM MgCl$_2$, pH 7.4; 30°C) with a Clark-type oxygen electrode. Mitochondria were suspended at 0.5 mg/ml, and electron transport was initiated by the addition of complex I (5 mM glutamate plus 2.5 mM malate) or complex II (10 mM succinate plus 1.25 µM rotenone) substrates. The rate of maximal coupled (state 3) respiration was then determined after adding 0.6 mM ADP. Mitochondrial functional integrity was assessed by the respiratory control ratio (RCR; ADP-stimulated/unstimulated respiration). In all measurements, the RCR values were >7.0 with glutamate/malate and >4.0 with succinate as electron donors, confirming functional intactness of isolated mitochondria.

Determination of aconitase activity
Mitochondrial aconitase activity was determined spectrophotometrically as described previously (Lapointe and Hekimi, 2008). In brief, citrate was used as the substrate of aconitase and the conversion of citrate into α-ketoglutarate in the presence of NADP$^+$-dependent isocitrate dehydrogenase was monitored by following the formation of NADPH at 340 nm. The reaction mixture of 1 ml contained 50 mM Tris-HCl, (pH 7.4, 30 mM sodium citrate, 0.5 mM MnCl$_2$, 0.2 mM NADP$^+$, and isocitrate dehydrogenase (2 U/ml). The reaction was started by addition of mitochondrial protein, and aconitase activity was calculated as nanomole of NADPH formed per minute per milligram of protein.

UQ$_{10}$ supplementation
Female $Mclk1^{+/+}$ and $Mclk1^{+/-}$ 3-mo-old mice from pure BALB/c background were randomly assigned to be fed either the control diet or UQ$_{10}$-enriched diet (2.81 mg/g) for 3 wk based on previously described protocol (Sumien et al., 2009). The UQ$_{10}$ that was used in diet preparation by Purina Mills Testdiet was provided by Tishcon corp. in the form of Q-gel liquid vehicle. Food intake was not affected by UQ$_{10}$ diet. Subsequently, mice were sacrificed and the amounts of UQ homologues (UQ$_9$ and UQ$_{10}$) were measured in homogenates, mitochondria, and mitochondrial subfractions from liver.

Electron transport chain assays
Mitochondrial samples were diluted with 30 mM potassium phosphate, pH 7.4, to reach a concentration of ∼1 mg/ml protein concentration and then subjected to three rounds of freezing-thawing. The rate of electron transport between complex I and complex III was assayed by following the reduction of cytochrome c at 550 nm in the reaction mix containing 30 mM potassium phosphate, pH 7.4, 100 µM NADH, and 2 mM KCN. Rotenone insensitive activity was determined by adding 2 µg/ml rotenone in the reaction mixture, and it was subtracted from the total activity (Lapointe and Hekimi, 2008). Complex II activity was measured by following the decrease in absorbance because of the coupled reduction of 2,6-dichlorophenolindophenol at 600 nm with 750 nm as the reference wavelength. The reaction mixture containing 50 mM potassium phosphate, pH 7.4, 20 mM succinate, and 5 mM MgCl$_2$ was preincubated with 15 µg of mitochondrial protein at 30°C. After 10 min of incubation, 2 µg antimycin, 2 µg rotenone, 2 mM KCN, and 150 µM 2,6-dichlorophenolindophenol were added. 2,6-Dichlorophenolindophenol can accept electrons from the complex II–bound endogenous ubiquinol or exogenous ubiquinol. Thus, the activity was first monitored for 1 min without the addition of exogenous ubiquinone. Subsequently, complex II activity was also measured with the addition of 100 µM ubiquinone (UQ$_1$) and was monitored for 2 min. All reactions were initiated by the addition of mitochondrial proteins.

Life span determination
Life span was determined in mouse cohorts comprising heterozygous mutants $Coq3^{+/-}$ and their wild-type littermate control. The number of days

that each mouse lived was recorded and graphed by the Kaplan-Meier method. Mice that died of apparent non-natural causes (e.g., cage fight injuries, pan flood accidents) were excluded from the longevity data.

Statistical analyses

Group data were presented as mean values ± SEM. Quantitative data were analyzed by GraphPad Prism Version 5.00 for Windows (Graph-Pad Software, Inc.). Comparisons between $Mclk1^{+/+}$ and $Mclk1^{+/-}$ were performed using an unpaired two-tailed Student's t test. For multiple comparisons, one-way ANOVA followed by Bonferroni's post hoc analysis was performed. For evaluating survival data, the log-rank (Mandel-Cox) test was performed. For all analyses, a value of $P < 0.05$ was considered significant.

Online supplemental material

Fig. S1 shows that overall mitochondrial UQ_{10} levels are normal in $Mclk1^{+/-}$ mice but display an altered distribution in OMs and IMs similar to that of UQ_9. Fig. S2 shows that $Coq3^{+/-}$ mice have no mitochondrial dysfunction, as indicated by normal levels of mitochondrial oxygen consumption and no change in mitochondrial aconitase activity. Both male and female $Coq3^{+/-}$ mice were found to have normal life spans. Fig. S3 shows that UQ_{10} supplementation has no significant effects on the whole liver and liver mitochondrial UQ_9 content of $Mclk1^{+/-}$ mice, but that accumulation of supplemented exogenous UQ_{10} in mutant $Mclk1^{+/-}$ mitochondria is greater than that in wild-type controls. Online supplemental material is available at http://www.jcb.org/cgi/content/full/jcb.201203090/DC1.

References

Beal, M.F. 2002. Coenzyme Q10 as a possible treatment for neurodegenerative diseases. *Free Radic. Res.* 36:455–460. http://dx.doi.org/10.1080/10715760290021315

Bentinger, M., K. Brismar, and G. Dallner. 2007. The antioxidant role of coenzyme Q. *Mitochondrion*. 7:S41–S50. http://dx.doi.org/10.1016/j.mito.2007.02.006

Bentinger, M., M. Tekle, and G. Dallner. 2010. Coenzyme Q—biosynthesis and functions. *Biochem. Biophys. Res. Commun.* 396:74–79. http://dx.doi.org/10.1016/j.bbrc.2010.02.147

Da Cruz, S., I. Xenarios, J. Langridge, F. Vilbois, P.A. Parone, and J.C. Martinou. 2003. Proteomic analysis of the mouse liver mitochondrial inner membrane. *J. Biol. Chem.* 278:41566–41571. http://dx.doi.org/10.1074/jbc.M304940200

Dai, Y.L., T.H. Luk, K.H. Yiu, M. Wang, P.M. Yip, S.W. Lee, S.W. Li, S. Tam, B. Fong, C.P. Lau, et al. 2011. Reversal of mitochondrial dysfunction by coenzyme Q10 supplement improves endothelial function in patients with ischaemic left ventricular systolic dysfunction: a randomized controlled trial. *Atherosclerosis*. 216:395–401. http://dx.doi.org/10.1016/j.atherosclerosis.2011.02.013

Dallner, G., and P.J. Sindelar. 2000. Regulation of ubiquinone metabolism. *Free Radic. Biol. Med.* 29:285–294. http://dx.doi.org/10.1016/S0891-5849(00)00307-5

DiMauro, S., C.M. Quinzii, and M. Hirano. 2007. Mutations in coenzyme Q10 biosynthetic genes. *J. Clin. Invest.* 117:587–589. http://dx.doi.org/10.1172/JCI31423

Ewbank, J.J., T.M. Barnes, B. Lakowski, M. Lussier, H. Bussey, and S. Hekimi. 1997. Structural and functional conservation of the *Caenorhabditis elegans* timing gene clk-1. *Science*. 275:980–983. http://dx.doi.org/10.1126/science.275.5302.980

Fato, R., S.D. Bernardo, E. Estornell, G. Parentic Castelli, and G. Lenaz. 1997. Saturation kinetics of coenzyme Q in NADH oxidation: rate enhancement by incorporation of excess quinone. *Mol. Aspects Med.* 18:S269–S273. http://dx.doi.org/10.1016/S0098-2997(97)00027-7

Fernández-Ayala, D.J., G. López-Lluch, M. García-Valdés, A. Arroyo, and P. Navas. 2005. Specificity of coenzyme Q10 for a balanced function of respiratory chain and endogenous ubiquinone biosynthesis in human cells. *Biochim. Biophys. Acta*. 1706:174–183. http://dx.doi.org/10.1016/j.bbabio.2004.10.009

Geromel, V., N. Darin, D. Chrétien, P. Bénit, P. DeLonlay, A. Rötig, A. Munnich, and P. Rustin. 2002. Coenzyme Q(10) and idebenone in the therapy of respiratory chain diseases: rationale and comparative benefits. *Mol. Genet. Metab.* 77:21–30. http://dx.doi.org/10.1016/S1096-7192(02)00145-2

Graham, J.M. 1993. Isolation of mitochondria, mitochondrial membranes, lysosomes, peroxisomes, and Golgi membranes from rat liver. *Methods Mol. Biol.* 19:29–40.

Graham, J.M. 2001a. Isolation of lysosomes from tissues and cells by differential and density gradient centrifugation. *Curr. Protoc. Cell Biol.* Chapter 3:3.6.

Graham, J.M. 2001b. Isolation of peroxisomes from tissues and cells by differential and density gradient centrifugation. *Curr. Protoc. Cell Biol.* Chapter 3:3.5.

Graham, J.M. 2001c. Purification of a crude mitochondrial fraction by density-gradient centrifugation. *Curr. Protoc. Cell Biol.* Chapter 3:3.4.

Green, D.E., and A. Tzagoloff. 1966. The mitochondrial electron transfer chain. *Arch. Biochem. Biophys.* 116:293–304. http://dx.doi.org/10.1016/0003-9861(66)90036-1

Guan, Z., M. Söderberg, P. Sindelar, S.B. Prusiner, K. Kristensson, and G. Dallner. 1996. Lipid composition in scrapie-infected mouse brain: prion infection increases the levels of dolichyl phosphate and ubiquinone. *J. Neurochem.* 66:277–285. http://dx.doi.org/10.1046/j.1471-4159.1996.66010277.x

Hsu, A.Y., W.W. Poon, J.A. Shepherd, D.C. Myles, and C.F. Clarke. 1996. Complementation of coq3 mutant yeast by mitochondrial targeting of the Escherichia coli UbiG polypeptide: evidence that UbiG catalyzes both O-methylation steps in ubiquinone biosynthesis. *Biochemistry*. 35:9797–9806. http://dx.doi.org/10.1021/bi9602932

Kalén, A., E.L. Appelkvist, T. Chojnacki, and G. Dallner. 1990. Nonaprenyl-4-hydroxybenzoate transferase, an enzyme involved in ubiquinone biosynthesis, in the endoplasmic reticulum-Golgi system of rat liver. *J. Biol. Chem.* 265:1158–1164.

Kamzalov, S., N. Sumien, M.J. Forster, and R.S. Sohal. 2003. Coenzyme Q intake elevates the mitochondrial and tissue levels of Coenzyme Q and alpha-tocopherol in young mice. *J. Nutr.* 133:3175–3180.

Kwong, L.K., S. Kamzalov, I. Rebrin, A.C. Bayne, C.K. Jana, P. Morris, M.J. Forster, and R.S. Sohal. 2002. Effects of coenzyme Q(10) administration on its tissue concentrations, mitochondrial oxidant generation, and oxidative stress in the rat. *Free Radic. Biol. Med.* 33:627–638. http://dx.doi.org/10.1016/S0891-5849(02)00916-4

Langsjoen, P.H., J.O. Langsjoen, A.M. Langsjoen, and L.A. Lucas. 2005. Treatment of statin adverse effects with supplemental Coenzyme Q10 and statin drug discontinuation. *Biofactors*. 25:147–152. http://dx.doi.org/10.1002/biof.5520250116

Lapointe, J., and S. Hekimi. 2008. Early mitochondrial dysfunction in long-lived Mclk1+/- mice. *J. Biol. Chem.* 283:26217–26227. http://dx.doi.org/10.1074/jbc.M803287200

Lapointe, J., Z. Stepanyan, E. Bigras, and S. Hekimi. 2009. Reversal of the mitochondrial phenotype and slow development of oxidative biomarkers of aging in long-lived Mclk1+/- mice. *J. Biol. Chem.* 284:20364–20374. http://dx.doi.org/10.1074/jbc.M109.006569

Lenaz, G., and M.L. Genova. 2009. Mobility and function of coenzyme Q (ubiquinone) in the mitochondrial respiratory chain. *Biochim. Biophys. Acta*. 1787:563–573. http://dx.doi.org/10.1016/j.bbabio.2009.02.019

Lenaz, G., G. Parenti Castelli, R. Fato, M. D'Aurelio, C. Bovina, G. Formiggini, M. Marchetti, E. Estornell, and H. Rauchova. 1997. Coenzyme Q deficiency in mitochondria: kinetic saturation versus physical saturation. *Mol. Aspects Med.* 18:S25–S31. http://dx.doi.org/10.1016/S0098-2997(97)00029-0

Levavasseur, F., H. Miyadera, J. Sirois, M.L. Tremblay, K. Kita, E. Shoubridge, and S. Hekimi. 2001. Ubiquinone is necessary for mouse embryonic development but is not essential for mitochondrial respiration. *J. Biol. Chem.* 276:46160–46164. http://dx.doi.org/10.1074/jbc.M108980200

Liu, X., N. Jiang, B. Hughes, E. Bigras, E. Shoubridge, and S. Hekimi. 2005. Evolutionary conservation of the clk-1-dependent mechanism of longevity: loss of mclk1 increases cellular fitness and lifespan in mice. *Genes Dev.* 19:2424–2434. http://dx.doi.org/10.1101/gad.1352905

López, L.C., C.M. Quinzii, E. Area, A. Naini, S. Rahman, M. Schuelke, L. Salviati, S. Dimauro, and M. Hirano. 2010. Treatment of CoQ(10) deficient fibroblasts with ubiquinone, CoQ analogs, and vitamin C: time- and compound-dependent effects. *PLoS ONE*. 5:e11897. http://dx.doi.org/10.1371/journal.pone.0011897

López-Martín, J.M., L. Salviati, E. Trevisson, G. Montini, S. DiMauro, C. Quinzii, M. Hirano, A. Rodriguez-Hernandez, M.D. Cordero, J.A. Sánchez-Alcázar, et al. 2007. Missense mutation of the COQ2 gene causes defects of bioenergetics and de novo pyrimidine synthesis. *Hum. Mol. Genet.* 16:1091–1097. http://dx.doi.org/10.1093/hmg/ddm058

Matthews, R.T., L. Yang, S. Browne, M. Baik, and M.F. Beal. 1998. Coenzyme Q10 administration increases brain mitochondrial concentrations and exerts neuroprotective effects. *Proc. Natl. Acad. Sci. USA*. 95:8892–8897. http://dx.doi.org/10.1073/pnas.95.15.8892

Nakai, D., S. Yuasa, M. Takahashi, T. Shimizu, S. Asaumi, K. Isono, T. Takao, Y. Suzuki, H. Kuroyanagi, K. Hirokawa, et al. 2001. Mouse homologue of coq7/clk-1, longevity gene in *Caenorhabditis elegans*, is essential for coenzyme Q synthesis, maintenance of mitochondrial integrity, and neurogenesis. *Biochem. Biophys. Res. Commun.* 289:463–471. http://dx.doi.org/10.1006/bbrc.2001.5977

Navarro, F., P. Navas, J.R. Burgess, R.I. Bello, R. De Cabo, A. Arroyo, and J.M. Villalba. 1998. Vitamin E and selenium deficiency induces expression of the ubiquinone-dependent antioxidant system at the plasma membrane. *FASEB J.* 12:1665–1673.

Norling, B., E. Glazek, B.D. Nelson, and L. Ernster. 1974. Studies with ubiquinone-depleted submitochondrial particles. Quantitative incorporation of small amounts of ubiquinone and its effects on the NADH and succinate oxidase activities. *Eur. J. Biochem.* 47:475–482. http://dx.doi.org/10.1111/j.1432-1033.1974.tb03715.x

Okado-Matsumoto, A., and I. Fridovich. 2001. Subcellular distribution of superoxide dismutases (SOD) in rat liver: Cu,Zn-SOD in mitochondria. *J. Biol. Chem.* 276:38388–38393. http://dx.doi.org/10.1074/jbc.M105395200

Preuss, H.G., B. Echard, D. Bagchi, D. Clouatre, and N.V. Perricone. 2010. Influence of gel and powdered formulations of coenzyme Q10 on metabolic parameters in rats. *Mol. Cell. Biochem.* 340:169–173. http://dx.doi.org/10.1007/s11010-010-0414-9

Quinzii, C.M., L.C. López, J. Von-Moltke, A. Naini, S. Krishna, M. Schuelke, L. Salviati, P. Navas, S. DiMauro, and M. Hirano. 2008. Respiratory chain dysfunction and oxidative stress correlate with severity of primary CoQ10 deficiency. *FASEB J.* 22:1874–1885. http://dx.doi.org/10.1096/fj.07-100149

Quinzii, C.M., L.C. López, R.W. Gilkerson, B. Dorado, J. Coku, A.B. Naini, C. Lagier-Tourenne, M. Schuelke, L. Salviati, R. Carrozzo, et al. 2010. Reactive oxygen species, oxidative stress, and cell death correlate with level of CoQ10 deficiency. *FASEB J.* 24:3733–3743. http://dx.doi.org/10.1096/fj.09-152728

Saito, Y., A. Fukuhara, K. Nishio, M. Hayakawa, Y. Ogawa, H. Sakamoto, K. Fujii, Y. Yoshida, and E. Niki. 2009. Characterization of cellular uptake and distribution of coenzyme Q10 and vitamin E in PC12 cells. *J. Nutr. Biochem.* 20:350–357. http://dx.doi.org/10.1016/j.jnutbio.2008.04.005

Salviati, L., E. Trevisson, M.A. Rodriguez Hernandez, A. Casarin, V. Pertegato, M. Doimo, M. Cassina, C. Agosto, M.A. Desbats, G. Sartori, et al. 2012. Haploinsufficiency of COQ4 causes coenzyme Q10 deficiency. *J. Med. Genet.* 49:187–191. http://dx.doi.org/10.1136/jmedgenet-2011-100394

Schneider, H., J.J. Lemasters, and C.R. Hackenbrock. 1982. Lateral diffusion of ubiquinone during electron transfer in phospholipid- and ubiquinone-enriched mitochondrial membranes. *J. Biol. Chem.* 257:10789–10793.

Sohal, R.S. 2004. Coenzyme Q and vitamin E interactions. *Methods Enzymol.* 378:146–151. http://dx.doi.org/10.1016/S0076-6879(04)78010-6

Sohal, R.S., and M.J. Forster. 2007. Coenzyme Q, oxidative stress and aging. *Mitochondrion.* 7:S103–S111. http://dx.doi.org/10.1016/j.mito.2007.03.006

Sohal, R.S., S. Kamzalov, N. Sumien, M. Ferguson, I. Rebrin, K.R. Heinrich, and M.J. Forster. 2006. Effect of coenzyme Q10 intake on endogenous coenzyme Q content, mitochondrial electron transport chain, antioxidative defenses, and life span of mice. *Free Radic. Biol. Med.* 40:480–487. http://dx.doi.org/10.1016/j.freeradbiomed.2005.08.037

Song, Y., Y. Hao, A. Sun, T. Li, W. Li, L. Guo, Y. Yan, C. Geng, N. Chen, F. Zhong, et al. 2006. Sample preparation project for the subcellular proteome of mouse liver. *Proteomics.* 6:5269–5277. http://dx.doi.org/10.1002/pmic.200500893

Sumien, N., K.R. Heinrich, R.A. Shetty, R.S. Sohal, and M.J. Forster. 2009. Prolonged intake of coenzyme Q10 impairs cognitive functions in mice. *J. Nutr.* 139:1926–1932. http://dx.doi.org/10.3945/jn.109.110437

Takahashi, M., M. Ogawara, T. Shimizu, and T. Shirasawa. 2012. Restoration of the behavioral rates and lifespan in clk-1 mutant nematodes in response to exogenous coenzyme Q(10). *Exp. Gerontol.* 47:276–279. http://dx.doi.org/10.1016/j.exger.2011.12.012

Tekle, M., M. Bentinger, T. Nordman, E.L. Appelkvist, T. Chojnacki, and J.M. Olsson. 2002. Ubiquinone biosynthesis in rat liver peroxisomes. *Biochem. Biophys. Res. Commun.* 291:1128–1133. http://dx.doi.org/10.1006/bbrc.2002.6537

Tomasetti, M., R. Alleva, B. Borghi, and A.R. Collins. 2001. In vivo supplementation with coenzyme Q10 enhances the recovery of human lymphocytes from oxidative DNA damage. *FASEB J.* 15:1425–1427.

Turunen, M., E. Swiezewska, T. Chojnacki, P. Sindelar, and G. Dallner. 2002. Regulatory aspects of coenzyme Q metabolism. *Free Radic. Res.* 36:437–443. http://dx.doi.org/10.1080/10715760290021298

Turunen, M., J. Olsson, and G. Dallner. 2004. Metabolism and function of coenzyme Q. *Biochim. Biophys. Acta.* 1660:171–199. http://dx.doi.org/10.1016/j.bbamem.2003.11.012

Wang, D., D. Malo, and S. Hekimi. 2010. Elevated mitochondrial reactive oxygen species generation affects the immune response via hypoxia-inducible factor-1alpha in long-lived Mclk1+/- mouse mutants. *J. Immunol.* 184:582–590. http://dx.doi.org/10.4049/jimmunol.0902352

Zheng, H., J. Lapointe, and S. Hekimi. 2010. Lifelong protection from global cerebral ischemia and reperfusion in long-lived Mclk1(+/)(-) mutants. *Exp. Neurol.* 223:557–565. http://dx.doi.org/10.1016/j.expneurol.2010.02.002